Biodegradable nano-films for capture and non-invasive release of circulating tumor cells

HHS Public Access

Author manuscript

Biomaterials. Author manuscript; available in PMC 2016 April 11.

Published in final edited form as:

Biomaterials. 2015 October ; 65: 93–102. doi:10.1016/j.biomaterials.2015.06.036.

Biodegradable nano-films for capture and non-invasive release of circulating tumor cells

Wei Li[#a,b], **Eduardo Reátegui**[#c,d], **Myoung-Hwan Park**[a], **Steven Castleberry**[a], **Jason Z. Deng**[a,e], **Bryan Hsu**[a], **Sarah Mayner**[a], **Anne E. Jensen**[d], **Lecia V. Sequist**[f,h], **Shyamala Maheswaran**[c,f], **Daniel A. Haber**[f,g,h], **Mehmet Toner**[c,d], **Shannon L. Stott**[d,f,h,**], and **Paula T. Hammond**[a,e,*]

[a] Department of Chemical Engineering, Massachusetts Institute of Technology, Cambridge, MA, USA

[b] Department of Chemical Engineering, Texas Tech University, Lubbock, TX, USA

[c] Department of Surgery, Harvard Medical School, Boston, MA, USA

[d] Center for Engineering in Medicine, Harvard Medical School, Boston, MA, USA

[e] David H. Koch Institute of Integrative Cancer Research, Massachusetts Institute of Technology, Cambridge, MA, USA

[f] Massachusetts General Hospital Cancer Center, Harvard Medical School, Boston, MA, USA

[g] Howard Hughes Medical Institute, Chevy Chase, MD, USA

[h] Department of Medicine, Harvard Medical School, Boston, MA, USA

[#] These authors contributed equally to this work.

Abstract

Selective isolation and purification of circulating tumor cells (CTCs) from whole blood is an important capability for both clinical medicine and biological research. Current techniques to perform this task place the isolated cells under excessive stresses that reduce cell viability, and potentially induce phenotype change, therefore losing valuable information about the isolated cells. We present a biodegradable nano-film coating on the surface of a microfluidic chip, which can be used to effectively capture as well as non-invasively release cancer cell lines such as PC-3, LNCaP, DU 145, H1650 and H1975. We have applied layer-by-layer (LbL) assembly to create a library of ultrathin coatings using a broad range of materials through complementary interactions. By developing an LbL nano-film coating with an affinity-based cell-capture surface that is capable of selectively isolating cancer cells from whole blood, and that can be rapidly degraded on command, we are able to gently isolate cancer cells and recover them without compromising cell viability or proliferative potential. Our approach has the capability to overcome practical hurdles

[*] Corresponding author. Department of Chemical Engineering, Massachusetts Institute of Technology, Cambridge, MA, USA. hammond@mit.edu (P.T. Hammond).. [**] Corresponding author. Center for Engineering in Medicine, Harvard Medical School, Boston, MA, USA. sstott@mgh.harvard.edu (S.L. Stott)..

Appendix A. Supplementary data

Supplementary data related to this article can be found at http://dx.doi.org/10.1016/j.biomaterials.2015.06.036.

and provide viable cancer cells for downstream analyses, such as live cell imaging, single cell genomics, and *in vitro* cell culture of recovered cells. Furthermore, CTCs from cancer patients were also captured, identified, and successfully released using the LbL-modified microchips.

Keywords

Biodegradable; Nano-film; Alginate; Circulating tumor cells; Layer-by-layer; Surface modification

1. Introduction

Circulating tumor cells (CTCs) present in the bloodstream of patients with cancer, originate from primary or metastatic tumor sites, and are thought to mediate the hematogenous spread of cancer to distant sites [1–4]. Technological hurdles have limited their isolation and characterization because these cells are extremely rare (1 in 10^9 blood cells) and mixed with normal blood components [5]. Isolation of CTCs is of great interest in the scientific community due to their usefulness in analyzing the diagnosis and treatment of patients with epithelial cancers in lieu of invasive biopsies. In order to capture CTCs from the bloodstream, multiple isolation approaches have been discovered thus far, which in general, take advantage of differences in physical cell properties or known cell surface markers [4–10].

Methods for CTC capture and release can be separated into macro- and micro-processes. The former group includes density gradient centrifugation [11], microfiltration [12–14], and use of antibody-modified magnetic beads [15–18]. Examples of the latter include use of lectin-modified microposts [19–21], DNA aptamers attached to silicon nanowires [22–24], antibody-modified photolabile linkers on glass substrates [25,26], APBA-functionalized multi-walled carbon nanotube films [27,28], interaction between calmodulin with a calmodulin-binding peptide in the presence of calcium, and cryogels [29]. Despite these many approaches, there remain several issues with the release processes that must be addressed to realize the full potential of CTCs as a diagnostic and research tool. First, the cells must be viable; unfortunately, many existing methods exhibit lower than acceptable yields in the release of unharmed living cells. Second, the phenotype of the cells must be preserved in order to accurately study the cells. Stresses from shear force, non-physiologic temperature variation, aggressive reagents such as trypsin and UV exposure are known to affect the phenotype of captured cells [6,30,31]. In addition, the method must achieve both high cell recovery as well as high cell purity. Finally, the method must be feasible for disposable point-of-care use even in remote areas; it must not require excessive lab equipment, or be limited to electrical and optical means of cell detachment.

We present a new method of capture and release of CTCs using a microfluidic device, the ^{HB}CTC-chip [1,3], modified with enzymatically degradable nano-films that are conjugated with antibodies to a variety of specific cell surface markers. We show that layer-by-layer (LbL) [32–35] assembly as an effective method to coat nanometer scale film inside microfluidic devices with complex microstructures. We achieved 80% capture efficiency and 95% release efficiency for spiked prostate cancer cells with heterogeneous levels of

expression of the surface antigen EpCAM, as well as CTCs in the blood samples of patients with metastatic lung cancer. The viability of released cells was demonstrated to be ~90%. For the patient samples tested, CTCs were detected, captured and successfully released using the biomaterial coated-microchip we developed. The CTCs in the patient blood samples were found to range from 3.4 to 4.9 CTCs/mL, while less than 0.5 CTCs/mL was found in control samples.

2. Materials and methods

2.1. Materials

Alginate (ALG) (Pronova UPMVG, 60% guluronate, 40% mannuronate, M_w = 120 k and 280 k) was purchased from Novamatrix, Norway. Hyaluronic acid (HA, M_w = 200 k), poly(allylamine hydrochloride) (PAH, M_w = 60 k), poly-L-lysine (PLL, M_w = 50 k to 70 k), low molecular weight chitosan (LMWC, M_w = 15 k), diethylaminoethyl dextran (DEAED, M_w = 500 k) and all other reagents were purchased from Sigma Aldrich, USA.

2.2. Fabrication of herringbone CTC chip (^{HB}CTC-chip)

Negative photoresist (SU-8, MicroChem) was photolithographically patterned on silicon wafers to create masters with two-layer features [3]. The first layer is the main microfluidic channel and the second layer forms the herringbone structures. The heights of SU-8 features are ranging from 25 to 75 μm on the masters. Polydimethylsiloxane (PDMS, SYLGARD 184, Dow Corning) was poured, degassed, and cured in a conventional oven at 75 °C for 24 h. The cured PDMS replicas were removed from the molds, oxygen plasma treated, and bonded to glass substrates to form the final devices.

2.3. Biotin modification of ALG and HA

Alginate and hyaluronic acid were modified with biotin hydrazide (Sigma B7639) using standard carbodiimide reaction [36]. Briefly, 1.0 wt% of ALG or HA solution was prepared in MES buffer, pH = 6.0. Per 50 mL of ALG or HA solution, 80 mg of biotin hydrazide, 360 mg of 1-ethyl-3-[3- dimethylaminopropyl] carbodiimide hydrochloride (EDC, Pierce 22980), and 204 mg of hydroxysulfosuccinimide (Sulfo-NHS, Pierce 24510) were added and reacted for 3 h, after which time the solution was dialyzed against deionized H_2O for 48 h and lyophilized. Alginate or hyaluronic acid was reconstituted at 2 mg/mL in deionized H_2O prior to use.

2.4. Preparation of nano-films

Lay-by-Layer (LbL) assembly of charged polymers were applied to build nanofilms inside microfluidic devices [37]. Biotin modified ALG and HA were used to prepare anionic polymer solution, while PAH, PLL, LWMC and DEAED were used to prepare cationic polymer solutions. The initial experiments were performed using a simplified microfluidic device comprising a straight PDMS microchannel with the dimension of 400 μm (width) × 100 μm (height) × 10 mm (length) sealed on a glass substrate. Briefly, glass substrate was treated with oxygen plasma for 5 min and immediately bonded to oxygen plasma treated PDMS replicas to form final devices. For LbL assembly of nano-films, a cationic polymer solution (2 mg/mL) was first injected into the inlet of the device to occupy all the inside

area, sit for 5 min for the absorption of polymers, then the solution was removed by air flow and the device was washed with 1 mL DI water for two times, then subsequent anionic polymer solution (2 mg/mL) was injected into the device and allowed a 5 min absorption time, after which the device was washed with DI water. This process was repeated 5 times at room temperature under sterile conditions.

2.5. Degradation of nano-films

To visualize the degradation of nano-films, a solution of 0.05 mg/mL Streptavidin Dylight 650 fluorescent conjugates (Thermo Scientific) in PBS was introduced into the modified microchannels and stored at 4 °C for 4 h. Then the avidin solutions were removed and the devices were washed thoroughly with DI water. The fluorescent intensity of each film was recorded using a fluorescent-optical microscope (BX53, Olympus) at the same exposure time of 2 s. A 2 mg/mL enzyme solution (alginate layse or hyaluronate lyase in PBS containing 1 wt% bovine serum albumin, BSA) was introduced into the microchannel and kept flowing for 30 min at 2.5 mL/h. After thoroughly washing the microchannel with DI water, the fluorescent intensity of the film was recoded using the same exposure time of 2 s. All the images were analyzed using ImageJ (NIH), and the fluorescent intensities of different types of films were normalized to the maximum intensity, which was obtained from ALG/LMWC film before degradation. The change (%) of FI before and after degradation was calculated by comparing the change of normalized value of FI over the initial FI for all the film compositions.

2.6. Optimization of the degradation of ALG/PAH nano-film

A series of ALG/PAH nano-films were made using the method described above. Four types of 2 mg/mL ALG solutions were prepared as following: ALG with molecular weight of 132 k at pH 4.5 and pH 7.2, as well as ALG with molecular weight of 280 k at pH 4.5 and 7.2. PAH used in this experiment was labeled with fluorescein. Film thickness was measured using an optical surface profilometer (Dektak 150, Veeco). Fluorescent intensities of four types of films were recorded at t = 0, 10 min, 20 min, and 30 min. The degradation efficiency (%) was calculated by comparing the change of FI over the initial FI. The morphology of films before and after degradation was determined using Atomic Force Microscopy (Dimension 3100, Bruker).

2.7. Surface modification of ^{HB}CTC-chips with ALG/PAH nano-film

The surface of the inside wall of ^{HB}CTC-chips was modified with ALG/PAH nano-films through Lay-by-Layer (LbL) assembly as described above. Glass substrate was treated with oxygen plasma for 5 min and immediately bonded to oxygen plasma treated PDMS replicas to form final devices. Briefly, PAH solution (2 mg/mL, pH 4.5) was first injected into the inlet of the device to occupy all the inside area, sit for 5 min for the absorption, then the solution was removed by air flow and the device was washed with 1 mL DI water for two times, then biotin modified ALG solution (2 mg/mL, pH 4.5) was injected into the device and allowed a 5 min absorption time, after which the device was washed with DI water. This process was repeated 5 times at room temperature under sterile conditions. A solution of 0.05 mg/mL Streptavidin in PBS was introduced into the device and stored in at 4 °C until use. Within 24 h of the experiment, 20 μg/mL biotinylated goat antihuman EpCAM (R&D

Systems) solution in PBS containing 1% BSA and 0.09% sodium azide were added to the devices. For coating IgG antibody, biotinylated normal goat IgG (R&D Systems) was in place of the biotinylated EpCAM. One hour prior to running the ^{HB}CTC-chip, devices were purged with 3% BSA with 0.05% Tween20 (Fisher Scientific) solution.

2.8. Cell line preparation

A human prostate cancer cell line, PC-3 (ATCC, VA), were cultured at 37 °C in F-12K growth medium containing 1.5 mM L-glutamine supplemented with 10% FBS and 1% Penicillin/Streptomycin with media changes every two days. Human prostate cancer DU 145 and LNCaP (ATCC, VA), were cultured according to the protocols from ATCC. Cells were released from culture flasks through incubation in 0.05% Trysin- EDTA (Invitrogen, CA) at 37 °C for 5 min. Prior to spiking into whole blood, all cells were labeled with a fluorescent cellular dye (CellTracker™ Orange, Invitrogen, CA) following the manufacturers' protocol. The cell suspension was subsequently diluted to the desired concentration. Experiments were performed using PC-3 cells suspended in serum-free medium or spiked into healthy donor whole blood. For the mixed cancer cell population capture and release experiment, prior to spiking into whole blood, each cell line was labeled with a different fluorescent cellular dye (CellTracker™ Blue, Red or Green, Invitrogen, CA). A mixture of cells was spiked into whole blood with the concentration of each cell line of 5000/mL. Experiments were performed similarly to the method described above. Lung cancer cell lines H1975 and H1650 were cultured with RPMI Medium 1640 and supplemented with 10% FBS under similar conditions described above.

2.9. Cell capture and release

Spiked cell experiments in whole blood were performed with either the single channel devices or ^{HB}CTC-chips. Experiments with the ^{HB}CTC-chips were processed with the standard CTC processing machine [1]. Large ^{HB}CTC-chips were subsequently imaged and enumerated using automated image-processing system ((Eclipse 90i, Nikon, Melville, NY) under 10× magnification). All device preparations and processing conditions for the ^{HB}CTC-chips were run as previously described. Capture efficiency was calculated as the number of spiked cells captured in the ^{HB}CTC-chip divided by the total number of cells flowed through the device. For the releasing experiment, the device was first washed with PBS, then the alginate lyase (2 mg/mL) in PBS containing 1% BSA was flowed through the device using a syringe pump (PHD 2200, Harvard Apparatus). The cell collection vial containing cell media was connected at the outlet of the device. Both cells remaining on the microfluidic device and in the collection vials were imaged and counted manually on a fluorescence microscope. Recovered cell viability was measured using a standard Live/Dead fluorescent assay (Life Technologies L3224) and compared to control cells that were never introduced into the microfluidic devices.

2.10. Immunostaining

Captured cells on were fixed with 4% paraformaldehyde and washed with PBS immediately following blood processing. The fixed cells were permeabilized with 1% NP40 and blocked with 2% normal goat serum/3% BSA before the addition of primary antibodies for immunostaining. The primary antibodies used for CTC targeting were rabbit wide spectrum

anti-cytokeratin (1:100, abcam), rabbit anti-MET (1:1000, BD Biosciences), anti-SOX2 (1:50, BD Biosciences) and anti-EGFR (1:200, BD Biosciences). Anti-CD45 mIgG1 (1:100, BD Biosciences) was added to target white blood cells. Next, secondary immunofluorescent labeled antibodies were added to amplify the signal along with DAPI to label the nuclei. The secondary antibodies used were goat anti-rabbit Alexa Flour 488 (1:200, Jackson) and goat anti-mouse IgG1 Alexa Flour 594 (1:200, Jackson). Following staining, the devices were washed with PBS and stored at 4 °C until microscopy imaging. Released CTCs were immobilized on poly-L-lysine coated glass slides for 15 min prior to the staining protocol.

2.11. Study subjects and blood processing

Patients with advanced lung cancer were recruited according to a protocol approved by the institutional review board (IRB) at Massachusetts General Hospital. Blood specimens from healthy volunteers were collected under a separate IRB-approved protocol. Metastatic lung cancer patients treated at the Massachusetts General Hospital Cancer Center donated 10–20 mL of blood on one or more occasions for analysis on the ^{HB}CTC-chip per our IRB protocol. All specimens were collected into Vacutainer (Becton–Dickinson) tubes containing the anticoagulant EDTA and were processed through the ^{HB}CTC-chip within 6 h of blood draw. Samples were run on the previously described microfluidic processing machine [3]. Briefly, a 5 mL aliquot of blood was placed in an air-tight conical tube on a rocker assembly, and blood was pneumatically driven through the chip at a flow rate of 1.5 mL/h. Then, the ^{HB}CTC-chips were flushed with 2.5 mL of PBS at 2.5 mL/h to remove any nonspecifically bound cells.

3. Results

3.1. Design of LbL nano-films for capture and release of CTCs

The Herringbone (HB) CTC-chip design [3] consists of a glass slide (25 mm × 75 mm) bonded to a polydimethylsiloxane (PDMS) substrate, containing eight microchannels with patterned herringbone structures on their upper surface [3]. The internal walls of the device are coated with nano-films that can be further functionalized with antibodies against EpCAM or other protein molecules. The overall height of the channel is 50 μm and the height of the HB grooves is 40 μm. As shown in Fig. 1a, cancer cells from whole blood were captured due to the interactions of EpCAM on the cell membrane surface with the antibodies that were conjugated on the wall of the devices. After capture of the CTCs, an enzyme solution was introduced into the device that rapidly degrades the nano-film, causing the CTCs to detach from the surface of the internal walls. The nano-film coated surface on the wall of the ^{HB}CTC-chip was formed through layer-by-layer (LbL) assembly of oppositely charged polyelectrolytes. The anionic polymers, alginate (ALG) or hyaluronic acid (HA), were modified with biotin groups through the conjugation of the free acids on the polyelectrolyte backbone with N-(3- aminopropyl) methacrylamide hydrochloride using standard carbodiimide coupling chemistry, in the presence of biotin hydrazide (Supporting Information Fig. S1). The biotin group can be used to conjugate EpCAM antibodies or other relevant antibodies against relevant tumor cell markers to the LbL film surface via biotin-avidin linkers after the formation of the LbL films. Various cationic polymers (polyallylamine hydrochloride (PAH), poly-L-lysine (PLL), low molecular weight chitosan

(LWMC), and diethylaminoethyl dextran (DEAED)) were used to prepare LbL films with ALG or HA. The degradation of LbL films was achieved by exposure to bacterial enzymes (alginate lyase for ALG-based films and hyaluronidase for HA-based films, respectively), which cleave the backbone of the biopolymers [36]. Subsequently, captured cells detach from the surface upon the degradation and dissolution of the LbL films (Fig. 1a). Fig. 1b shows the interface between the captured cell and the LbL film. To visualize the formation of LbL films and the conjugation of streptavidin on the surface of ^{HB}CTC-chips, we used fluorescent-labeled polymer (FITC-PAH, in green color) and Avidin-DyLight 650 (in red color) for the initial testing. As shown in Fig. 1c, fluorescent microscope images in the green channel confirm that a smooth thin film was coated onto the surface inside the ^{HB}CTC-chip, and the colocalization of green and red signal indicate that the avidin linkages were successfully conjugated onto the LbL film.

3.2. Formation and degradation of LbL nano-films

As shown in Fig. 2a, each of the two anionic polymers ALG and HA was paired with one each of the following group of cationic polymers (PAH, PLL, LWMC, and DEAED) to form LbL nano-films on the inner walls of the ^{HB}CTC-chip. A preliminary test was performed in a simplified chip with one straight microfluidic channel sealed onto glass slide; the purpose of this study was to determine film compositions that would form uniform films and undergo significant degradation over a pre-determined timeframe. All films were made by repeating the deposition process five times during film preparation to generate five bilayers, followed by the adsorption of fluorescently labeled streptavidin, which binds to the biotin linker.

Fluorescent microscope images of eight different LbL film formulations are shown in Fig. 2b, and the fluorescent intensity (FI) of each film before and after degradation was recorded and analyzed by ImageJ. Among these eight types of films, the ALG/LMWC film has the strongest FI, which was set as the maximum value of 100 and used to normalize the fluorescent intensity of other films. The images of the films made by ALG/PAH, ALG/PLL, ALG/LMWC, HA/PAH and HA/PLL indicate uniform fluorescence across the surface, suggesting that the films are smoothly and conformally coated onto the surface. The images of the films made by ALG/DEAED, HA/LWMC and HA/DEAED yielded noticeably large variations in fluorescent intensity in different areas on the surface, which indicates that the LbL films are not uniform for those three conditions. It is anticipated that the film breakdown would be dependent on the relative composition of the polyelectrolytes used and the assembly conditions. As shown in Fig. 2c, among those eight types of films, ALG/PAH film was found to have the largest change (67.7%) in the fluorescent intensity before and after degradation; for the purpose of fast release of cells from the film-coated surface, we chose ALG/PAH film for further optimization.

3.3. Biodegradation of ALG/PAH LbL nano-films

Four types of ALG/PAH nano-films were further investigated to optimize the degradation of those films. Specifically, the films were prepared by varying the molecular weight (M_w = 132 k or 280 k) of alginate polymer and the pH of alginate solutions (pH = 4.5 or 7.2) used for LbL assembly, with consistent molecular weight of FITC labeled PAH at 60 k; the pH of PAH solutions were kept at 4.5. As shown in Fig. 3a, the fluorescent intensity of all four

types of films decreased gradually as increasing the exposure time to enzyme solution from 10 to 30 min, indicating those films underwent progressive degradation. The thicknesses of the films before degradation were determined by optical surface profilometer, and ranged from 25 nm to 40 nm (Fig. 3b). The fluorescence intensity changes of those films were recorded and the degradation efficiency was plotted at various time points. As shown in Fig. 3c, over 50% of the ALG(280 k)/pH4.5 film was degraded in the first 10 min, and the film continually degraded over 70% after 20 min and then slowly degraded to up to 75% in 30 min. From the Atomic Force Microscopy images shown in Fig. 3d and e, the ALG (280 k)/pH4.5 film has a smooth surface with a surface roughness of 3.1 nm before degradation, while the surface roughness (RMS) increased to 5.5 nm and the film displayed a porous surface morphology after degradation.

3.4. Capture and release of spiked prostate and lung cancer cell lines

The capture and release of spiked prostate (PC-3, n = 3) and lung (H1650 and H1975, n = 3) cancer cells in whole blood was carried out on PAH/ALG modified ^{HB}CTC-chips. As shown in Fig. 4a, the image illustrates uniform blood flow in the device. The ^{HB}CTC-chip was scanned using an automated fluorescent microscopy system after washing out the non-bonded cells, and the captured cells were recorded (shown in Fig. 4a) and counted. The capture efficiency was calculated to be 79.2% (prostate) and 78.9% (lung), which is similar to the capture efficiency that was achieved using non-degradable GMBS modified ^{HB}CTC-chips [3]. The total number of non-specifically captured cells platform (i.e. CD45+ cells and DAPI only cells) was also determined using our microscopy platform, allowing us to calculate an average on-chip purity of 53% for our spiked cell experiments. More importantly, over 95% of captured cells were successfully released from the ^{HB}CTC-chip in 30 min after flushing with an enzyme solution at the flow rate of 2.5 mL/h (Fig. 4c). Lower release efficiency was observed when decreasing flushing time or reducing the flow rate of enzyme solution to 1.0 mL/h. EpCAM (green) expression on the surface of PC-3 cells was confirmed by immunofluorescent staining, as shown in Fig. 4d for captured PC-3 cells and released PC-3 cells in Fig. 4e. Released cells also contained leukocytes and other types of blood cells, which were positive for CD45 (red) staining (Fig. 4f).

3.5. Cell viability of the released PC-3 cells

The viability of released cells was measured by a Live/Dead assay (Fig. 5a). The number of viable PC-3 cells in the mixture of blood cells was counted and compared to the total numbers of PC-3 cells that were captured on the ^{HB}CTC-chip. Cell viability (%) was close to 90% after cells were released and cultured in a petri dish for 30 min and decreased slightly to 88% after 2 h in culture at room temperature, which is similar to the cell viability of the control cells that did not go through the capture-release cycle (Fig. 5b). More importantly, released cells were cultured at 37 °C with 5% CO_2 for 5 days; following this period, they readily adhere to the surfaces of the culture plate and proliferate, suggesting that the cells were not damaged after being captured and released. A hint of orange fluorescent signal on the cell surface (Fig. 5c) also suggests that those cells were originally stained and spiked into whole blood, as the fluorescent signal can retain in cells for three to six generations.

3.6. Capture and release of mixed cancer cell populations spiked into blood

Three types of human prostate cancer cell lines LNCaP, DU 145 and PC-3 were stained with three different cell tracker fluorescent dyes, and spiked into blood samples. Using flow cytometry, the number of each type of cell in blood can be easily quantified (Fig. 6a). As shown in Fig. 6b, three types of prostate cancer cells were captured using the ALG/PAH modified ^{HB}CTC-chip. The relative intensity of the fluorescent signal in each channel is approximately 1:1:1, which is similar to the ratio used for spiking the blood. Fig. 6c is a representative heat map showing the distribution of captures of these three types of cells across an entire ^{HB}CTC-chip. Captured cells are observed throughout the entire chip, regardless of cell type. The density of captured cells is slightly higher at the top and bottom side of the chip than that in the center area of the chips. More quantitative data from the flow cytometer shows that the ratio of the three types of cells was maintained at approximately 1:1:1 (the same as the initial spike ratio), which confirms that the capture and release process did not change the relative population of cell types in the blood.

3.7. Capture and release of CTCs from patient samples

The ALG/PAH modified ^{HB}CTC-chips were also used to isolate CTCs in blood samples of patients with metastatic lung cancer. To account for the heterogeneity that may exist within patient derived CTCs, the ^{HB}CTC-chips were conjugated with antibodies against EpCAM, as well as EGFR, and HER2, which are commonly expressed in lung and other epithelial cancers [38]. As shown in Fig. 7a, the identity of CTCs was confirmed by their positive expression of EpCAM, HER2 and MET as shown with a green fluorescent signal, in combination with the lack of expression of any red fluorescent signal for the blood cell leukocyte marker CD45. Fig. 7b is the micrograph of the same cell as shown in Fig. 7a, after release from the ^{HB}CTC-chip, indicating little or no change in cell shape or morphology. Fig. 7c shows the capture and release of cells from blood samples of lung cancer patients and healthy donors as controls. For four patient samples tested, the ALG/PAH ^{HB}CTC-chip isolated from 2.4 to 5.9 CTCs/ml, while less than 0.5 similarly stained cells/ml were found in control blood samples drawn from healthy individuals. This result is in agreement with previous studies [1–3].

4. Discussion

We previously demonstrated the effectiveness of microfluidic chips in capturing EpCAM-expressing cells using antibody-coated microstructures [1,3]. Efficient cell capture was validated using cancer cells spiked into control blood and clinical blood samples from patients with prostate cancer [39]. However, for those previous studies, the captured CTCs could not be noninvasively released from the surface of the device, limiting the use of CTCs in functional assays and single cell sequencing. In the present work, we present a biodegradable nano-film that conformally coats the interior surfaces of the microfluidic ^{HB}CTC-chip, and can achieve high capture efficiency but also release of the captured cells without sacrificing the viability of the cells. The nano-film was constructed from the layer-by-layer (LbL) assembly of weakly charged polyelectrolytes with opposite charges [32,33]. In particular, at least one of the film components was a native biological charged polysaccharide by design. This component of the film was readily functionalized

with biotin linkers via free acid side groups, enabling simple conjugation with antibodies against a variety of cancer cell surface markers.

Specific antigen–antibody interactions between the cancer cells and the inner surface of the ^{HB}CTC-chip ensure high capture efficiencies, which is in good agreement with our previous studies [2,3]. More importantly, the nano-film coating on the inner wall of ^{HB}CTC-chip can undergo degradation over short time periods through exposure of the surface to mild natural enzyme solutions that breakdown the polysaccharide film component within 30 min [36]. The degradation of the nano-film led to the near-quantitative release of the captured cancer cells from the ^{HB}CTC-chip. As illustrated schematically in Fig. 1a, small fragments of the nano-film may remain attached to the surface of the released cell, which was observed in fluorescence microscopy images (Fig. S2); the presence of small patches of film do not appear to prevent the adhesion, expansion and colonization of these cells, or to change any of the cell markers or characteristics, and in separate studies, similar kinds of LbL “backpacks” have been found to have no effect on final cell function [40]. LbL assembly is a unique and highly efficient means of constructing thin conformal nanoscale thin films on the inner wall of the ^{HB}CTC-chips; it enables the tuning of key functionalities such as degradation rate and antibody presentation while enabling the coating of complex microstructures within microfluidic devices (Fig. 1c) [37].

To ensure prompt degradation of the nano-film upon exposure to the enzyme solution, the sacrificial layers created inside the ^{HB}CTC-chip must be uniformly coated throughout the entire inner surface of the device. For this purpose, we studied the film formation and degradation of a library of film compositions, and the film composition with the best performance (smooth conformal coating and maximum degradation ratio) was chosen for further optimization (Fig. 2). The degradation kinetics of the polymer nano-film depends on the film thickness, charge density of the polyelectrolytes, effective mesh size of the polymer network, etc. For the ALG/PAH film, the higher molecular weight of ALG in the film and lower charge density of ALG (as alginate has a pk_a close to 3.5, ALG polymer in a pH 4.5 solution is less charged than that in a pH 7.2 solution) resulted a slightly thicker film with a looser ionically crosslinked polymer network [41,42]. As a result, faster degradation and better degradation efficiency were achieved for coatings prepared under the above conditions (shown in Fig. 3b and c). On the other hand, the degradation of LbL coatings was also affected by the flow rate and the exposure time of enzyme solutions applied on the film surface. Since the release efficiency is directly correlated to the film degradation, we achieved over 95% cell release efficiency at 2.5 mL flushing rate in 30 min (Fig. 4c). To prevent damage to the CTCs due to high shear forces, flushing flow rates greater than 2.5 mL/h were avoided. As for capturing CTCs, previous studies set a benchmark for optimal capture efficiencies using both spiked CTCs samples and patient blood samples [1–3]. When compared to our previously published performance data for the ^{HB}CTC-chip with the original non-degradable GMBS linkers, the LbL-nano coating modified ^{HB}CTC-chip maintained similar capture efficiencies (Fig. 4b), which suggests that a thin sacrificial nano-coating did not affect the interactions between antigen molecules on the cell surface and enabled sufficient presentation of anti-EpCAM antibodies on the surface of ^{HB}CTC-chip.

Affinity based capture of CTCs in microfluidic devices has been shown to provide valuable clinical information for cancer diagnosis, protein expression of cells, and cancer cell genomics [2,3,10,43–45]. However, these approaches for rare-cell isolation use irreversible attachment for the capture antibodies, introducing practical hurdles for downstream analysis where viable CTCs are required (such as live cell imaging, single cell genomics, and *in vitro* cell culture of recovered cells). Our LbL nano-coating modified ^{HB}CTC-chips can capture cancer cells with the same efficiency, but release live cells under very mild conditions and preserve high cell viability while maintaining cellular characteristics of the captured CTCs. As shown in Fig. 5b, the cancer cells that went through capture-release cycles have the same viability as the cancer cells that were stored in tissue culture microplates. Furthermore, the released cells can grow and proliferate under normal *in vitro* cell culture conditions for weeks (Fig. 5c). Previous studies have shown heterogeneity of CTCs in terms of their size, shape, and the density of EpCAM molecules on their surface [1,46,47]. For this study, we investigated the versatility of our ^{HB}CTC-chips for the capture and release of a mixed population of spiked prostate cancer cell lines (LNCaP, PC-3, and DU 145). To match the phenotype of our patient sample co-hort, spiked lung cancer cell lines (H1650 and H1975) were also tested using our methods. Our device showed efficient, simultaneous capture of all five cell lines regardless of size (shown in Fig. 6b and c, Fig. S5) and EpCAM expression [46]. Spiking 5000 cancer cells into 1 mL of whole blood, we were able to achieve an average of 80% capture efficiency while maintaining an on-chip purity of 53%. Although this purity value is more than sufficient for downstream molecular analysis of cancer cell lines [3], it may not be readily translatable to clinical samples since the exact number of CTCs present in a patient sample is unknown. Therefore, approaches that allow for the release and recovery of CTCs in solution are of extreme value since additional isolation strategies (e.g. single cell micromanipulation) can be used to investigate CTCs at the single cell level [48]. As such, we have achieved uniform, viable release of these five cancer cell lines (Fig. 6d, Fig. S6), demonstrating the that our release approach is independent of the number of bound surface antigens and should be amenable to several different tumor cell types.

To test the true clinical utility of our system, blood samples from metastatic non-small cell lung cancer patients were used to test our LbL-modified ^{HB}CTC-chips. Due to the unknown level of heterogeneity of surface antigens for lung patient CTCs, the ^{HB}CTC-chips were conjugated with a cocktail of capture antibodies (i.e. EpCAM, HER2, EGFR). This antibody-cocktail method has shown great success for capturing patient CTCs from our previous studies [38]. We were able to identify lung CTCs captured on the chip, as well as trace the same cell after it is released (Fig. 6a and b). CTCs were detected and identified for all the patient samples we investigated (Fig. 6c, n = 4). Although the number of clinical samples was limited, the number of CTCs released was comparable to the number captured on the device, suggesting minimal cell loss during the process. The CTCs are directly available following release without any additional steps for further downstream analyses.

5. Conclusions

In summary, we reported a novel approach for capturing and noninvasively releasing CTCs using microfluidic ^{HB}CTC-chips modified with biodegradable nano-films that conjugated

with antibodies to a variety of specific cell surface markers. Nanometer-scale films inside microfluidic devices with complex microstructures were created by layer-by-layer (LbL) assembly. Our ^{HB}CTC-chips show 80% of capture efficiency and 95% of release efficiency for both single spiked prostate cancer cells and a mixture of cancer cell lines with variable EpCAM expression of surface markers. Our noninvasive release strategy can preserve cell viability to close to 90%. Using LbL-modified ^{HB}CTC-chips, CTCs from metastatic lung cancer patients were captured, identified and released. Our approach is ready amenable to translation on ^{HB}CTC-chips that are currently used for clinical applications, and can also be translated to a range of different device surfaces, from silicon and glass to plastic or paper, to generate low-cost detection devices.

Supplementary Material

Refer to Web version on PubMed Central for supplementary material.

Acknowledgments

We express our gratitude to the all patients who participated in this study and the healthy volunteers who contributed blood samples. We are also grateful to Dr. Ajay Shah for initial critical discussions. We would like to acknowledge Octavio Hurtado and Laura Libby for their expert technical support. This work was supported by a grant from Stand Up to Cancer, a joint program of the Entertainment Industry Foundation (EIF) and the American Association for Cancer Research (AACR). We acknowledge support from: National Institute for Biomedical Imaging and Bioengineering (NIBIB) EB008047 (M. T., and D.A.H.), and NIH P41 EB002503-11 (M. T.).

References

1. Nagrath S, Sequist LV, Maheswaran S, Bell DW, Irimia D, Ulkus L, et al. Isolation of rare circulating tumour cells in cancer patients by microchip technology. Nature. 2007; 450:1235–1U10. [PubMed: 18097410]
2. Yu M, Stott S, Toner M, Maheswaran S, Haber DA. Circulating tumor cells: approaches to isolation and characterization. J. Cell Biol. 2011; 192:373–382. [PubMed: 21300848]
3. Stott SL, Hsu CH, Tsukrov DI, Yu M, Miyamoto DT, Waltman BA, et al. Isolation of circulating tumor cells using a microvortex-generating herring-bone-chip. Proc. Natl. Acad. Sci. U. S. A. 2010; 107:18392–18397. [PubMed: 20930119]
4. Chen YC, Li P, Huang PH, Xie YL, Mai JD, Wang L, et al. Rare cell isolation and analysis in microfluidics. Lab Chip. 2014; 14:626–645. [PubMed: 24406985]
5. Yap TA, Lorente D, Omlin A, Olmos D, de Bono JS. Circulating tumor cells: a multifunctional biomarker. Clin. Cancer Res. 2014; 20:2553–2568. [PubMed: 24831278]
6. Alix-Panabieres C, Pantel K. Technologies for detection of circulating tumor cells: facts and vision. Lab Chip. 2014; 14:57–62. [PubMed: 24145967]
7. Alix-Panabieres C, Pantel K. Circulating tumor cells: liquid biopsy of cancer. Clin. Chem. 2013; 59:110–118. [PubMed: 23014601]
8. Balic M, Williams A, Lin H, Datar R, Cote RJ. Circulating tumor cells: from bench to bedside. Annu. Rev. Med. 2013; 64:31–44. [PubMed: 23092385]
9. Doyen J, Alix-Panabieres C, Hofman P, Parks SK, Chamorey E, Naman H, et al. Circulating tumor cells in prostate cancer: a potential surrogate marker of survival. Crit. Rev. Oncol. Hematol. 2012; 81:241–256. [PubMed: 21680196]
10. Haber DA, Velculescu VE. Blood-based analyses of cancer: circulating tumor cells and circulating tumor DNA. Cancer Discov. 2014; 4:650–661. [PubMed: 24801577]
11. Gertler, R.; Rosenberg, R.; Fuehrer, K.; Dahm, M.; Nekarda, H.; Siewert, JR. Detection of circulating tumor cells in blood using an optimized density gradient centrifugation. In: Allgayer,

H.; Heiss, MM.; Schildberg, FW., editors. Molecular Staging of Cancer, Springer-Verlag Berlin. Berlin: 2003. p. 149-155.

12. Zheng SY, Lin HK, Lu B, Williams A, Datar R, Cote RJ, et al. 3D microfilter device for viable circulating tumor cell (CTC) enrichment from blood. Biomed. Microdevices. 2011; 13:203–213. [PubMed: 20978853]
13. Karabacak NM, Spuhler PS, Fachin F, Lim EJ, Pai V, Ozkumur E, et al. Microfluidic, marker-free isolation of circulating tumor cells from blood samples. Nat. Protoc. 2014; 9:694–710. [PubMed: 24577360]
14. Zhang ZF, Xu J, Hong B, Chen XL. The effects of 3D channel geometry on CTC passing pressure - towards deformability-based cancer cell separation. Lab a Chip. 2014; 14:2576–2584.
15. Dharmasiri U, Witek MA, Adams AA, Soper SA. Yeung ES, Zare RN. Microsystems for the capture of low-abundance cells. Annual Review of Analytical Chemistry. 2010; 3:409–431.
16. Di Corato R, Bigall NC, Ragusa A, Dorfs D, Genovese A, Marotta R, et al. Multifunctional nanobeads based on quantum dots and magnetic nano-particles: synthesis and cancer cell targeting and sorting. ACS Nano. 2011; 5:1109–1121. [PubMed: 21218823]
17. Durgadas CV, Sharma CP, Sreenivasan K. Fluorescent and super-paramagnetic hybrid quantum clusters for magnetic separation and imaging of cancer cells from blood. Nanoscale. 2011; 3:4780–4787. [PubMed: 21956754]
18. Fu AH, Wilson RJ, Smith BR, Mullenix J, Earhart C, Akin D, et al. Fluorescent magnetic nanoparticles for magnetically enhanced cancer imaging and targeting in living subjects. ACS Nano. 2012; 6:6862–6869. [PubMed: 22857784]
19. Vickers DAL, Hincapie M, Hancock WS, Murthy SK. Lectin-mediated microfluidic capture and release of leukemic lymphocytes from whole blood. Biomed. Microdevices. 2011; 13:565–571. [PubMed: 21455756]
20. Xie M, Hu J, Long YM, Zhang ZL, Xie HY, Pang DW. Lectin-modified tri-functional nanobiosensors for mapping cell surface glycoconjugates. Biosens. Bioelectron. 2009; 24:1311–1317. [PubMed: 18790631]
21. Zheng T, Yu HM, Alexander CM, Beebe DJ, Smith LM. Lectin-modified microchannels for mammalian cell capture and purification. Biomed. Microdevices. 2007; 9:611–617. [PubMed: 17516171]
22. Chen L, Liu XL, Su B, Li J, Jiang L, Han D, et al. Aptamer-mediated efficient capture and release of T lymphocytes on nanostructured surfaces. Adv. Mater. 2011; 23:4376. [PubMed: 21882263]
23. Shen QL, Xu L, Zhao LB, Wu DX, Fan YS, Zhou YL, et al. Specific capture and release of circulating tumor cells using aptamer-modified nanosubstrates. Adv. Mater. 2013; 25:2368–2373. [PubMed: 23495071]
24. Zhao WA, Cui CH, Bose S, Guo DG, Shen C, Wong WP, et al. Bioinspired multivalent DNA network for capture and release of cells. Proc. Natl. Acad. Sci. U. S. A. 2012; 109:19626–19631. [PubMed: 23150586]
25. Shin DS, Seo JH, Sutcliffe JL, Revzin A. Photolabile micropatterned surfaces for cell capture and release. Chem. Commun. 2011; 47:11942–11944.
26. Wang PF, Hu HY, Wang Y. Novel photolabile protecting group for carbonyl compounds. Org. Lett. 2007; 9:1533–1535. [PubMed: 17371037]
27. Sada T, Fujigaya T, Niidome Y, Nakazawa K, Nakashima N. Near-IR laser-triggered target cell collection using a carbon nanotube based cell-cultured substrate. ACS Nano. 2011; 5:4414–4421. [PubMed: 21627128]
28. Yoon HJ, Kozminsky M, Nagrath S. Emerging role of nanomaterials in circulating tumor cell isolation and analysis. ACS Nano. 2014; 8:1995–2017. [PubMed: 24601556]
29. Colinas RJ, Walsh AC. Cell separation based on the reversible interaction between calmodulin and a calmodulin-binding peptide. J. Immunol. Methods. 1998; 212:69–78. [PubMed: 9671154]
30. Zheng Q, Iqbal SM, Wan Y. Cell detachment: post-isolation challenges. Biotechnol. Adv. 2013; 31:1664–1675. [PubMed: 23978676]
31. Born C, Zhang Z, Alrubeai M, Thomas CR. Estimation of disruption of animal-cells by laminar shear-stress. Biotechnol. Bioeng. 1992; 40:1004–1010. [PubMed: 18601208]
32. Hammond PT. Building biomedical materials layer-by-layer. Mater. Today. 2012; 15:196–206.

33. Hammond PT. Engineering materials layer-by-layer: challenges and opportunities in multilayer assembly. Aiche J. 2011; 57:2928–2940.
34. Boudou T, Crouzier T, Ren KF, Blin G, Picart C. Multiple functionalities of polyelectrolyte multilayer films: new biomedical applications. Adv. Mater. 2010; 22:441–467. [PubMed: 20217734]
35. Decher G. Fuzzy nanoassemblies: toward layered polymeric multicomposites. Science. 1997; 277:1232–1237.
36. Shah AM, Yu M, Nakamura Z, Ciciliano J, Ulman M, Kotz K, et al. Biopolymer system for cell recovery from microfluidic cell capture devices. Anal. Chem. 2012; 84:3682–3688. [PubMed: 22414137]
37. Castleberry SA, Li W, Deng D, Mayner S, Hammond PT. Capillary flow layer-by-layer: a microfluidic platform for the high-throughput assembly and screening of nanolayered film libraries. ACS Nano. 2014; 8:6580–6589. [PubMed: 24836460]
38. Yu M, Bardia A, Wittner BS, Stott SL, Smas ME, Ting DT, et al. Circulating breast tumor cells exhibit dynamic changes in epithelial and mesenchymal composition. Science. 2013; 339:580–584. [PubMed: 23372014]
39. Stott SL, Hsu C-H, Tsukrov DI, Yu M, Miyamoto DT, Waltman BA, et al. Isolation of circulating tumor cells using a microvortex-generating herring-bone-chip. Proc. Natl. Acad. Sci. 2010; 107:18392–18397. [PubMed: 20930119]
40. Doshi N, Swiston AJ, Gilbert JB, Alcaraz ML, Cohen RE, Rubner MF, et al. Cell-based drug delivery devices using phagocytosis-resistant backpacks. Adv. Mater. 2011; 23:H105–H109. [PubMed: 21365691]
41. Mendelsohn JD, Barrett CJ, Chan VV, Pal AJ, Mayes AM, Rubner MF. Fabrication of microporous thin films from polyelectrolyte multilayers. Langmuir. 2000; 16:5017–5023.
42. Shiratori SS, Rubner MF. pH-dependent thickness behavior of sequentially adsorbed layers of weak polyelectrolytes. Macromolecules. 2000; 33:4213–4219.
43. Miyamoto DT, Sequist LV, Lee RJ. Circulating tumour cells-monitoring treatment response in prostate cancer. Nat. Rev. Clin. Oncol. 2014; 11:401–412. [PubMed: 24821215]
44. Yu M, Bardia A, Wittner B, Stott SL, Smas ME, Ting DT, et al. Circulating breast tumor cells exhibit dynamic changes in epithelial and mesenchymal composition. Science. 2013; 339:580–584. [PubMed: 23372014]
45. Maheswaran S, Sequist LV, Nagrath S, Ulkus L, Brannigan B, Collura CV, et al. Detection of mutations in EGFR in circulating lung-cancer cells. N. Engl. J. Med. 2008; 359:366–377. [PubMed: 18596266]
46. Rao CG, Chianese D, Doyle GV, Miller MC, Russell T, Sanders RA, et al. Expression of epithelial cell adhesion molecule in carcinoma cells present in blood and primary and metastatic tumors. Int. J. Oncol. 2005; 27:49–57. [PubMed: 15942643]
47. Poczatek RB, Myers RB, Manne U, Oelschlager DK, Weiss HL, Bostwick DG, et al. Ep-CAM levels in prostatic adenocarcinoma and prostatic intraepithelial neoplasia. J. Urol. 1999; 162:1462–1466. [PubMed: 10492238]
48. Reátegui E, Aceto N, Lim EJ, Sullivan JP, Jensen AE, Zeinali M, Martel JM, Aranyosi AJ, Li W, Castleberry S, Bardia A, Sequist LV, Haber DA, Maheswaran S, Hammond PT, Toner M, Stott SL. Tunable nanostructured coating for the capture and selective release of viable circulating tumor cells. Adv. Mater. 2015; 27:1593–1599. [PubMed: 25640006]

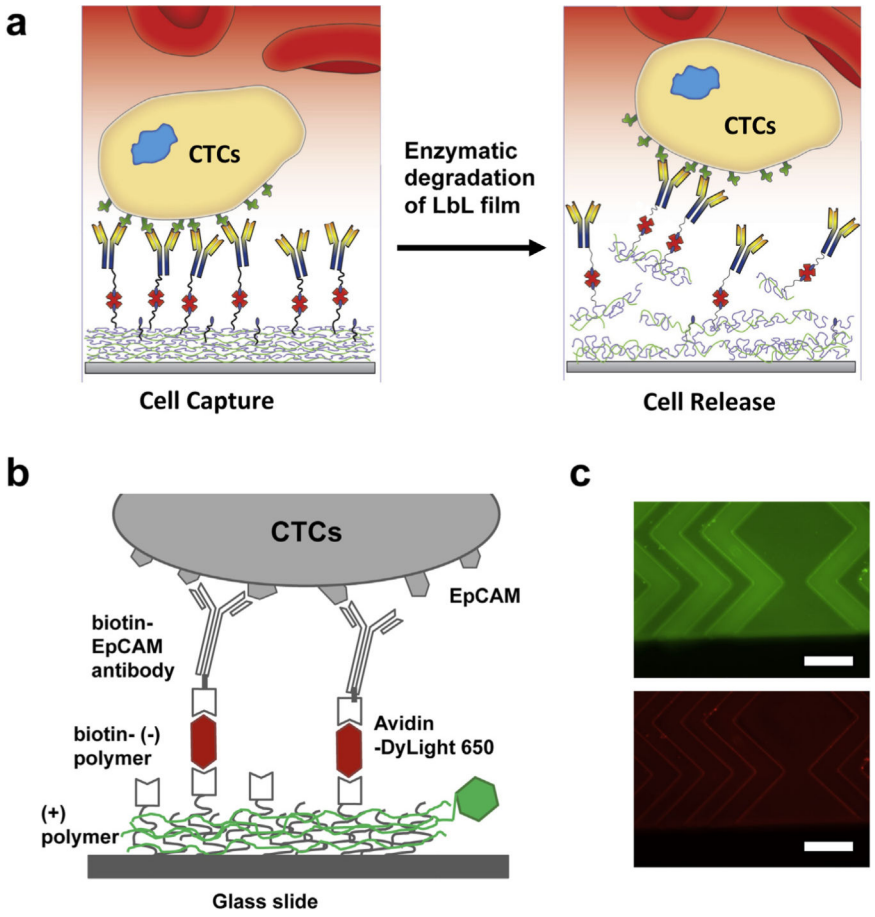

Fig. 1.

Design of the nano-film for the capture and release of CTCs. (a) Schematics of capturing and releasing of CTCs using microfluidic ^{HB}CTC-chips modified with enzymatically degradable LbL nano-film coating. (b) Schematics of the interface between the functionalized surface of ^{HB}CTC-chip and surface of CTCs. (c) The structure of ^{HB}CTC-chip and fluorescent microscope images showing the surface of ^{HB}CTC-chip modified with the LbL film and the avidin binding linkages, in green and red color, respectively. The black area at the bottom of the image is where the PDMS substrate sealed to glass slide. The scale bar is 100 μm.

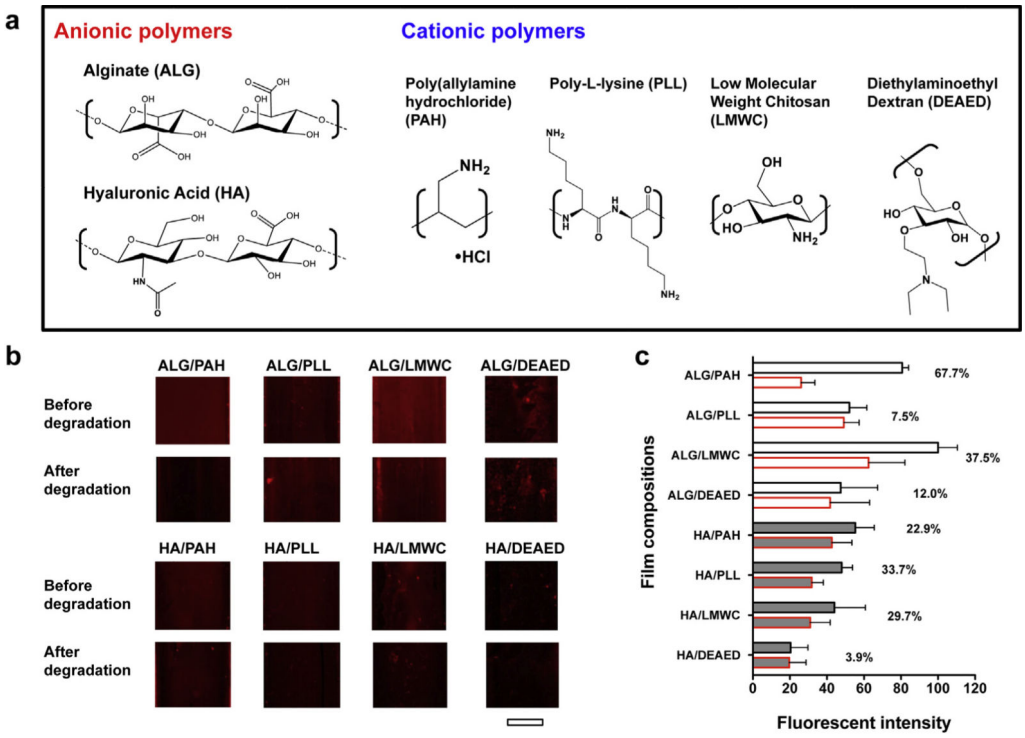

Fig. 2.

Formation and degradation of LbL nano-films. (a) The molecular structures of anionic polymers and cationic polymers used. (b) Representative fluorescent images of LbL nano-films before and after degradation. The scale bar is 200ìm. The degradation of the films was conducted by flowing an enzyme solution in the film-coated microchannel for 30 min at a flow rate of 2.5 mL/h. The scale bar is 200 μm. (c) The change of FI of the films before and after degradation. FI of all films was normalized by the FI of ALG/LMWC film before degradation, which was used as the maximum value of 100. Bars with a black box and a red box represent FI of films before and after degradation, respectively. Bars filled with white and gray color represent FI of films made by ALG and HA, respectively. The values of the change (%) of FI after the degradation of films are listed beside the bars.

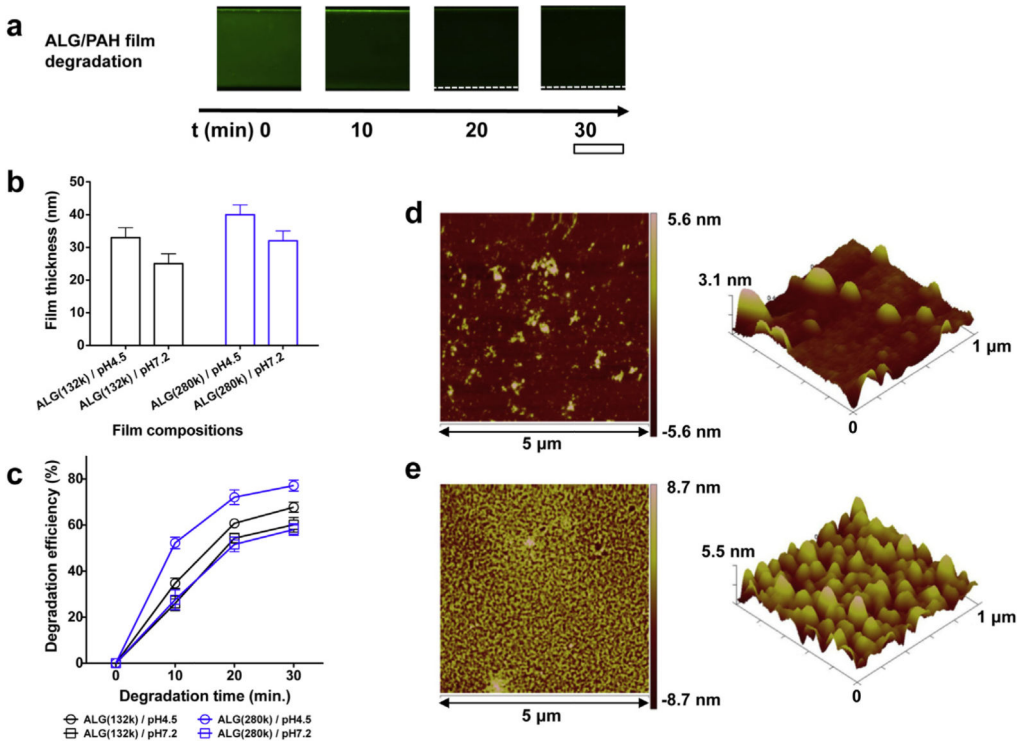

Fig. 3.

Enzymatic degradation of ALG/PAH LbL films. (a) Optical fluorescent images of ALG/PAH LbL films at various time of degradation. The white dash lines were added at the edge of the film for eye guidance. The scale bar is 200 μm. (b) and (c) Film thickness and degradation of ALG/PAH LbL films made by various experimental conditions, respectively. 2D (d) and 3D (e) Atomic Force Microscopy images of ALG/PAH LbL films before and after degradation, respectively. The film was made using ALG (280 k)/PAH at pH 4.5 for ALG solution. RMS roughness of the film was 3.1 nm before degradation and 5.5 nm after degradation.

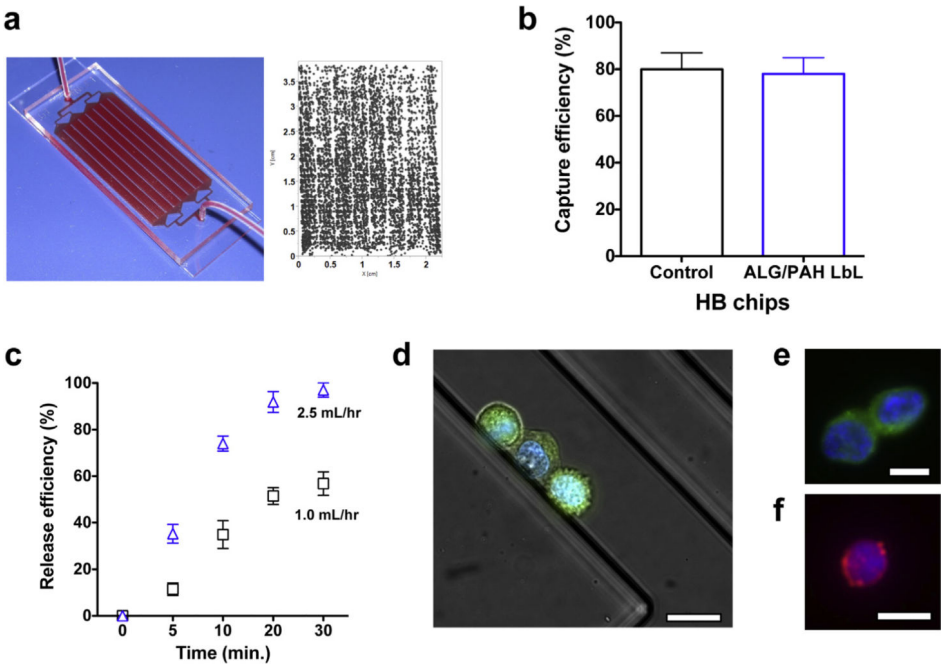

Fig. 4.

Capture and release of spiked PC-3 cells. (a) Left: optical image of whole blood flowing through an ^{HB}CTC-chip. The concentration of spiked PC-3 cells in whole blood was 5000/mL. Right: image shows a representative distribution of captured cells (shown as black dots) in the ^{HB}CTC-chip. The scale bar is 10 mm. (b) Capture efficiency of ALG/PAH modified ^{HB}CTC-chip in comparison with conventional ^{HB}CTC-chip. (c) Release efficiency at various degradation times and flow rates of enzyme solution. (d)–(f) Immunofluorescent staining of cell surface receptors for captured PC-3 cells in the ^{HB}CTC-chip (d), released PC-3 cells (e), and white blood cells (f), shown here is EpCAM expression in green, DAPI nuclear staining in blue, and CD45 expression in red. The scale bars are 20μm.

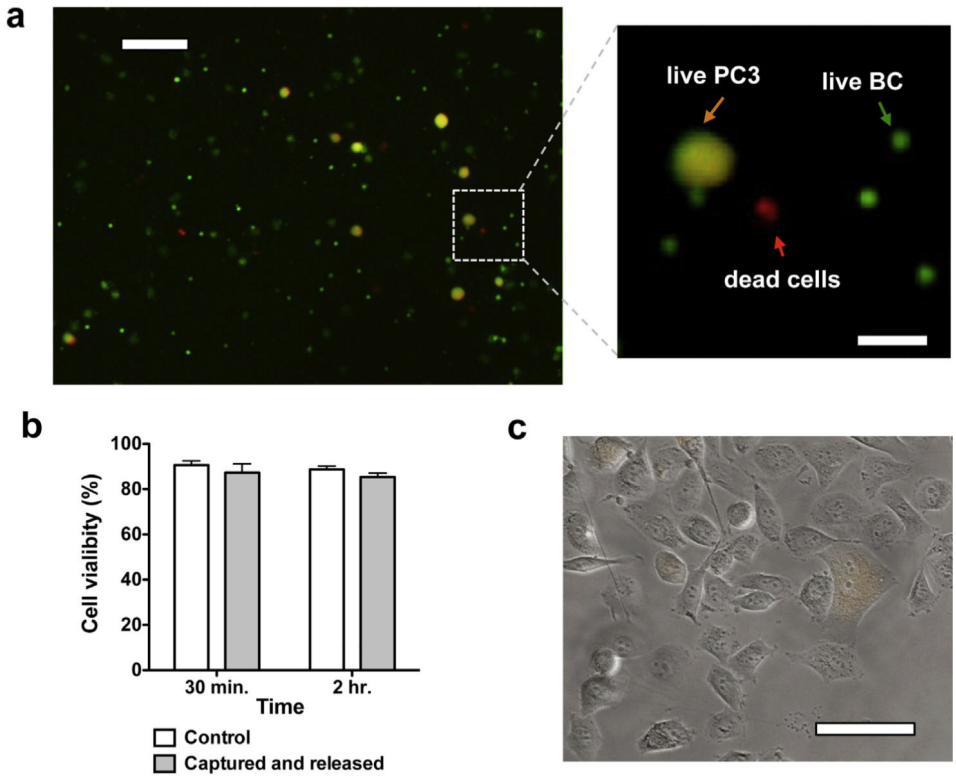

Fig. 5.

Cell viability of released PC-3 cells. (a) The viability of released cells were evaluated using a fluorescent LIVE (green)/DEAD (red) assay. PC-3 cells were pre-stained with cell tracker orange before spiking into blood. Live PC-3 cells show co-localization of orange and green colors. The scale bars are 100 ìm in the main image and 10 ìm for the zoom-in image, respectively. (b) Cell viability of PC-3 cells spiked in blood. White bars shown the control cells and gray bars shown captured and released cells. (c) Released PC-3 cells shown proliferation and maintained viable for culturing. Optical microscopy image was taken after five days of releasing from ^{HB}CTC-chip. The scale bar is 100 μm.

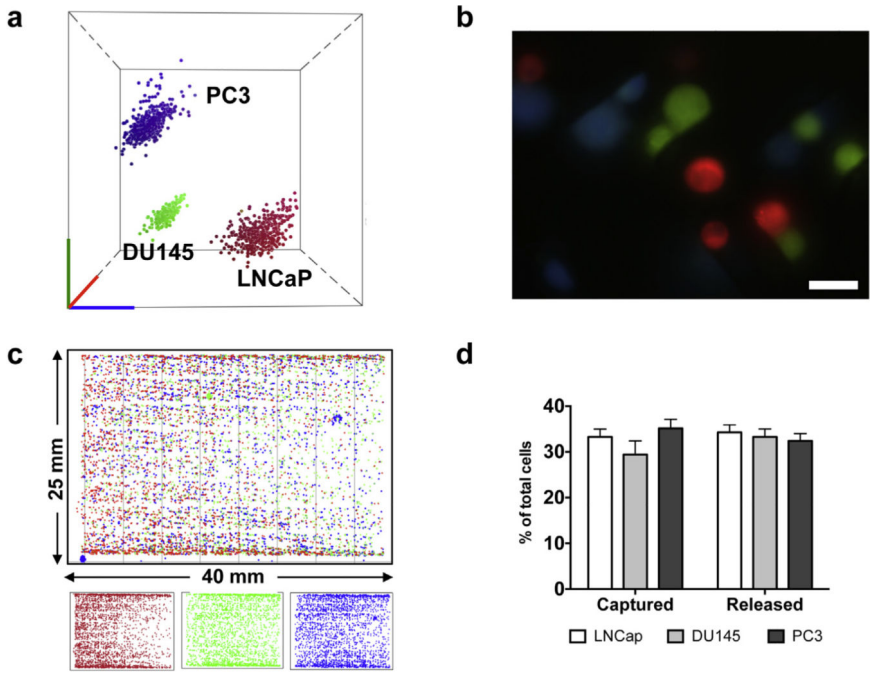

Fig. 6.

Capture and release of spiked populations of cancer cell lines. (a) A 3D flow cytometer image of three types of human prostate cancer cell lines that were stained with three different fluorescent dyes. Specifically, red for LNCaP cells, green for DU 145 cells and blue for PC-3 cells. (b) Representative fluorescent image of captured LNCaP, DU 145 and PC-3 cells, with the ratio of these three cell types of 1:1:1. The scale bar is 20 μm. (c) Representative heat map (top, combined with three florescent channels) and individual heat map (bottom) for single channel of an entire ^{HB}CTC-chip, showing the distribution of capture of LNCaP, DU 145 and PC-3 cells, from 2 mL of whole blood sample. (d) The percentages of these three types of cells that were captured on a ^{HB}CTC-chip, compared to those that were released from the ^{HB}CTC-chip and stored in a petri dish.

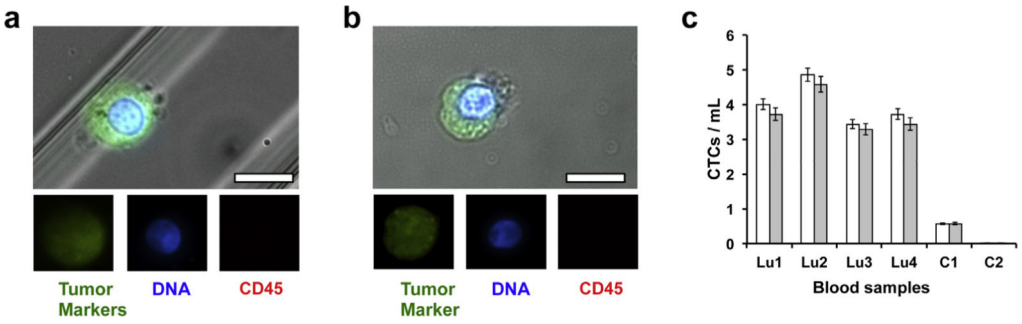

Fig. 7.

Capture and release of CTCs from patient blood samples. Immunofluorescent staining of cell surface receptors for captured CTC (a) and the corresponding released CTC (b) from patients with metastatic prostate cancer using ALG/PAH modified ^{HB}CTC-chip. Shown here are EpCAM, HER2 and MET expression in green, DAPI nuclear staining in blue, and CD45 expression in red. The scales bar is 20ìm. (c) CTCs captured and released in blood samples from four lung cancer patients (Lu1 to Lu4) and two healthy donors (C1 and C2) using ALG/PAH modified ^{HB}CTC-chips.